



# Thermodynamic analysis of fly ash nanofluid for automobile (heavy vehicle) radiators

Boopathi Palaniappan<sup>1</sup> · Venkatachalam Ramasamy<sup>1</sup>

Received: 23 June 2018 / Accepted: 16 October 2018 / Published online: 26 October 2018  
© Akadémiai Kiadó, Budapest, Hungary 2018

## Abstract

This paper presents the thermodynamic performance of automobile radiators using water (60%), ethylene glycol (40%)—fly ash nanofluids. The influence of nanofluid flow rate and concentration of fly ash on heat transfer parameters (such as overall heat transfer coefficient and heat transfer), energy transfer parameters (such as pumping power and performance index) and exergy performance parameters (such as exergy destruction rate and exergy efficiency) are studied. The results showed that the heat transfer characteristics, energy performance parameters and exergy performance parameters were significantly improved with increase in the concentration of fly ash in a base fluid (60% water–40% ethylene glycol) from 0.2 to 2% (by volume). The outcome of this research has the potential to replace conventional working fluids in heavy vehicle radiators. The concentration of fly ash with base fluid (60% water–40% ethylene glycol) was optimized to 2% (by volume).

**Keywords** Fly ash nanofluid · Automobile radiators · Thermodynamic analysis

## List of symbols

$A$	Heat transfer area ( $\text{m}^2$ )
$D_h$	Hydraulic diameter (m)
$E$	Total exergy
$H$	Height (m)
$Q$	Heat transfer rate (kW)
PI	Performance index
$\Delta p$	Pressure difference ( $\text{Nm}^{-2}$ )
$R$	Gas constant ( $\text{J kg}^{-1} \text{K}^{-1}$ )
$T$	Temperature (K)
$U$	Overall heat transfer coefficient ( $\text{W m}^{-2} \text{K}$ )
$\dot{V}$	Volume flow rate ( $\text{m}^3 \text{s}^{-1}$ )
$W$	Width (m)
$c_p$	Specific heat capacity ( $\text{J kg}^{-1} \text{K}^{-1}$ )
$d$	Diameter (m)
$f$	Friction factor
$h$	Convective heat transfer coefficient ( $\text{W m}^{-2} \text{K}$ )
$k$	Thermal conductivity ( $\text{Wm}^{-1}\text{K}^{-1}$ )
$L$	Length (m)
$\dot{m}$	Mass flow rate ( $\text{kg s}^{-1}$ )
$u$	Velocity ( $\text{m s}^{-1}$ )

## Greek letters

$\varepsilon$	Effectiveness
$\eta$	Efficiency
$\mu$	Dynamic viscosity ( $\text{Ns m}^{-2}$ )
$\phi$	Particle volume fraction
$\rho$	Mass density ( $\text{kg m}^{-3}$ )
$\sigma$	Stephan–Boltzmann constant ( $\text{W m}^{-2} \text{K}^{-4}$ )

## Subscription

a	Air
c	Coolant
bf	Base fluid
np	Nanoparticle
in	Inlet
out	Outlet

## Abbreviation

%vol	%Volume fraction
EG	Ethylene glycol
$Re$	Reynolds number

## Introduction

The multi-cylinder diesel engines in heavy vehicles produce high heat load and thermal stress in engine components. Earlier studies reported that about 8.5% of total

✉ Boopathi Palaniappan  
pboopathiphd10@gmail.com

<sup>1</sup> Department of Automobile Engineering, Institute of Road and Transport Technology, Erode, Tamil Nadu 638316, India

energy of the burned fuel inside the cylinder is transferred to the cylinder head by combustion gases and 50–65% heat carried by the cooling system is transferred through the cylinder head [1]. Most of the engine cylinder head thermal cracks and valve overheating have been occurred due to poor cooling performance [2]. The poor cooling performance of the engines directly affects the combustion efficiency, emission and durability of the engine components [3]. The cooling performance of the engine depends on the thermo-physical properties of engine coolant and their influence on heat transfer characteristics [4, 5].

The overall heat transfer coefficient, heat transfer rate and performance index of radiators are enhanced by nanofluids as a coolant. Mintsu et al. [6] tested with CuO/water and Al<sub>2</sub>O<sub>3</sub>/water nanofluids with different size nanoparticles in a cross-flow heat exchanger and reported that the addition of nanoparticles with water has improved thermo-physical properties and heat transfer rate. In another work, Peyghambarzadeh et al. [7] improved thermal performance of automobile radiators by about 45% with 1% of Al<sub>2</sub>O<sub>3</sub> nanoparticles (by volume) in pure water. Similarly, Nguyen et al. [8] reported that 6.8% Al<sub>2</sub>O<sub>3</sub> nanoparticles (by volume) in pure water has improved the thermal performance of a radiator by about 40%. Heris et al. [9] compared the thermal performance of CuO/water and Al<sub>2</sub>O<sub>3</sub>/water nanofluid coolants in a cross-flow heat exchanger. It was reported that heat transfer enhancement in nanofluids depends on type of particle, size of particle, base fluid, flow regime, thermal conductivity, boundary condition, nanoparticles chaotic movements, fluctuations and interactions. They also reported that Al<sub>2</sub>O<sub>3</sub>/water nanofluid has higher heat transfer enhancement when compared to CuO/water nanofluid. Li and Xuan [10] reported that about 20% increase in thermal performance with CuO/water nanofluid in automobile radiators. Vermahmoudi et al. [11] improved heat transfer rate by about 11.5% by 0.65% Fe<sub>2</sub>O<sub>3</sub> nanofluid (by volume) in a cross-flow heat exchanger. The research on SiO<sub>2</sub> nanoparticles dispersed in 40% water and 60% ethylene glycol (base fluid) was reported by Kulkarni et al. [12] and reported with 4.8% improvement of heat transfer with SiO<sub>2</sub> nanofluid when compared to base fluid. Murshed et al. [13] showed that about 33% enhancement of heat transfer in a radiator using 5% of TiO<sub>2</sub>-water nanofluid (by volume) with 10 nm size nanoparticles. Dinesh kumar et al. [14] made a review on preparation methods, characterization techniques, properties measurement and applications of nanofluids and reported that composite nanofluids containing more than one type of nanoparticles can be used as coolant for cross-flow, compact heat exchangers. Sozen et al. [15] reported that fly ash exhausted from thermal power plants has a mixture of metal oxides like Al<sub>2</sub>O<sub>3</sub>, Fe<sub>2</sub>O<sub>3</sub>, TiO<sub>2</sub>, SiO<sub>2</sub>, CaO and MgO in different

proportions, which could be used for preparing nanofluids suitable for heat exchanger applications. They proved that the fly ash nanoparticles with water have improved thermo-physical and frictional properties with good enhanced thermal performance in a parallel flow concentric tube heat exchanger.

Generally the performance of heat exchangers is analyzed in terms of energy and exergy analysis [16]. Energy analysis measures the quantity of heat transfer transferred through the radiator, and it takes no account of available energy wasted. Exergy analysis measures the destruction of available energy (irreversibility) during the heat transfer process in the radiator. The irreversibilities in the radiator are due to thermo-physical properties, flow properties and thermodynamic properties [17]. The external irreversibility is due to non-attainability of perfect insulation with reference to the surroundings. The internal irreversibility causes cold end and hot end of the radiator. The cold end is created by conduction of heat to radiator outlet. In the hot end of the radiator, the air after passing the radiator will not reach an inlet temperature of radiator coolant due to internal irreversibility. The outlet air of radiator has some potential to cool the radiator coolant, and this is called exergy available with the air. This exergy available is wasted into the atmosphere, and this is called exergy destruction of radiator due to temperature. The internal irreversibility is due to friction and finite temperature between the coolant and surrounding. Both internal and external irreversibilities cause exergy loss or exergy destruction in the radiator heat exchange process. The exergy destruction is related to entropy generation by Gouy–Stodola theorem [18] (irreversibility  $(I) = T_0 S_{gen}$ ). The entropy generation in any heat exchange process ( $S_{gen}$ ) contains entropy generation due to internal irreversibility, external irreversibility and entropy production. Exergy destruction is a useful tool for evaluating the irreversibilities associated with a heat exchange process [19].

## Objectives of the study

The main objectives of this study are to investigate the effect of fly ash nanofluid volume concentration, coolant Reynolds number on overall heat transfer coefficient, heat transfer rate, pumping power, frictional exergy destruction rate, thermal exergy destruction rate, total exergy destruction rate and second law efficiency of a heavy vehicle radiator which is using fly ash nanofluid as coolant with turbulent flow condition subjected to constant wall temperature.

## Materials and methods

### Preparation of fly ash nanofluid

The fly ash from a cogeneration power plant in M/s. Ponni Sugars (Erode) Ltd, Tamil Nadu, India, was collected with size range 10 μm, surface area ranges 550–850 m<sup>2</sup>/g and utilized to prepare fly ash nanofluid. The composition of fly ash on mass basis was alumina (21.96%), ferric oxide (6.48%), titanium oxide (1.03%), magnesium oxide (2.12%), silica (47.08%), calcium oxide (16.03%), sodium oxide (1.28%), sulfur trioxide (2.13%) and potassium oxide (0.93%). The fly ash was nanosized for an average of 50 nm by using Spex-8000 ball milling. The base fluid was prepared by mixing 60% deionized water, 40% ethylene glycol and 0.2% sodium dodecyl benzyl sulfonate (SDBS) dispersant by volume. The conventional coolant used in automobile cooling system contains 40–30% ethylene glycol in 60–70% deionized water. The addition of ethylene glycol in water reduces heat transfer properties, but improves freezing and boiling temperature range. The thermo-physical properties of fly ash nanoparticles and base fluid are given in Table 1. The two-step method was used to prepare fly ash nanofluid in which the nanoparticles were directly added to the base fluid and ultrasonic vibration was made to mix, stabilize the nanoparticles. The mass of fly ash particles added to the base fluid to prepare 0.2–2% volume nanofluids was obtained [20, 21] using Eq. (1).

$$\% \text{Volume concentration}(\phi) = \frac{\frac{m_{np}}{\rho_{np}}}{\frac{m_{np}}{\rho_{np}} + \frac{m_{bf}}{\rho_{bf}}} \times 100 \quad (1)$$

The dispersion stability of nanoparticles is improved by ultrasonic vibration process (QSonica, USA, power rating: 700 W, frequency: 20 kHz) for two hours. The prepared nanofluids have been undisturbed for 15 days for checking sedimentation, and notable sedimentation was not observed. Figure 1a, b shows the microstructure of the fly ash before size reduction and fly ash nanofluid (1% by volume). The stability of the nanofluid was tested by absorption spectrometer and zeta potential analyzer, respectively. The optimum nanoparticles % in base fluid is 2% and above which the dispersion stability starts decreasing [14].

### Thermo-physical properties of nanofluid

The thermo-physical properties of fly ash nanofluid are the main influencing factors of thermal, frictional and exergy performance of automobile cooling system. Thermo-physical properties such as thermal conductivity, density, dynamic viscosity and specific heat of base fluid and

**Table 1** Physical properties of base fluid and fly ash nanoparticles

Property	Base fluid (60% water + 40% ethylene glycol)	Fly ash nanoparticle
Specific heat ( $c_p$ )/ kJ kg <sup>-1</sup> K <sup>-1</sup>	3752	1084.50
Mass density ( $\rho$ )/ Kg m <sup>-3</sup>	1054	3014
Dynamic viscosity ( $\mu$ )/ N-s m <sup>-2</sup>	0.00235	–
Thermal conductivity ( $k$ )/W m <sup>-1</sup> K <sup>-1</sup>	0.416	45.35

nanofluids were experimentally measured by using the hot wire transient method (KD2 thermal properties analyzer, Decagon Devices Inc, USA), electronic weighing balance, capillary viscometer and differential scanning calorimeter. The loss of nanoparticles during testing was measured by finding variations in mass density and pH of the nanofluids before and after testing. There were no objectionable variations found in density and pH of nanofluids collected after the experiment. The measured thermo-physical properties of fly ash nanofluids were compared to base fluid as relative quantities which are shown in Fig. 2.

Effective density of nanofluid coolant is given by [21, 22]

$$\rho_c = (1 - \phi)\rho_{bf} + \phi\rho_{np} \quad (2)$$

Specific heat of nanofluid coolant is given by [21, 22]

$$(\rho_c c_{pc}) = (1 - \phi)(\rho_{bf} c_{pbf}) + \phi(\rho_{np} c_{pnp}) \quad (3)$$

Dynamic viscosity of nanofluid coolant is defined by [23]

$$\mu_c = \mu_{bf}(1 + 2.5\phi + 6.2\phi^2) \quad (4)$$

Thermal conductivity of nanofluid coolant with Brownian motion is obtained by [21, 22]

$$k_c = k_{bf} \left[ \frac{(k_{np} + 2k_{bf}) + 2\phi(k_{np} - k_{bf})}{(k_{np} + 2k_{bf}) - \phi(k_{np} - k_{bf})} \right] + 5 \times 10^4 \beta \phi \rho_{bf} c_{pbf} \sqrt{\frac{\sigma T}{\rho_{np} d_{np}}} f(T, \phi) \quad (5)$$

$$\text{where } \beta = 8.4407(100\phi)^{-1.07304} [21, 22] \quad (6)$$

$$f(T, \phi) = (2.8217 \times 10^{-2} \phi + 3.917 \times 10^{-3} \left( \frac{T}{T_{ref}} \right) + (-3.0669 \times 10^{-2} \phi - 3.91123 \times 10^{-3})) [21, 22] \quad (7)$$

**Fig. 1** **a** Microstructure of fly ash and **b** fly ash nanofluid (1% volume concentration)

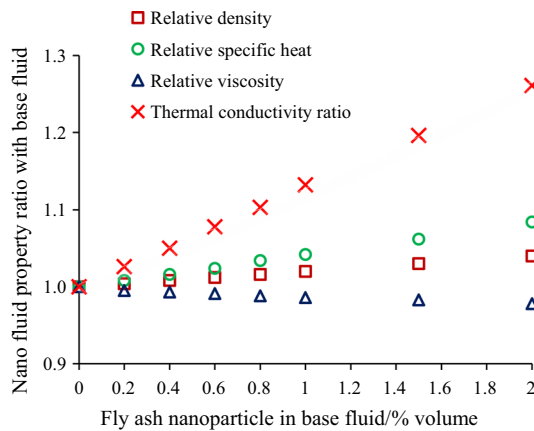
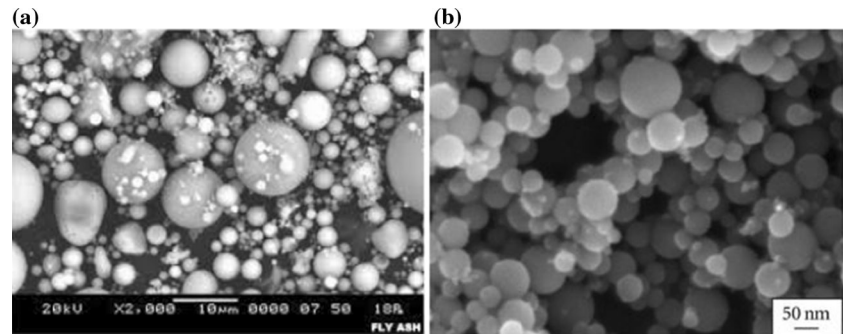


**Fig. 2** Relative physical properties of fly ash nanofluid with base fluid

## Experimental setup

The schematic layout of the experimental setup to do a thermodynamic analysis of fly ash nanofluid for automobile (heavy vehicle) radiator is shown in Fig. 3. The experimental setup consists of a HINO WO6D model, four stroke cycle, six cylinder, vertical in-line, water cooled, direct injection diesel engine (Capacity: 5.759 liters cubic capacity, 70 kW (95PS) output power @ 2400 rpm and 33 kgm torque @1600 rpm) with a hydraulic loading system and a closed circuit cooling system. The cooling system consists of engine cooling jacket connected with radiator (a compact heat exchanger [24], 194 elliptically cross-sectioned, vertical brass tubes in three zigzag rows and 171 continuous, parallel plate copper fins, brazed with lead and tin at the tube-fin joints), differential pressure transmitter, Coriolis mass flow meter (accuracy  $\pm 1\%$ ), two temperature sensors (PT 100RTD with range =  $-200$  to  $+850$  °C,  $\pm 0.15$  °C accuracy) at the inlet and outlet of radiator, flow control valve, coolant drain valve and connecting hoses. The air velocity, air inlet and outlet temperatures were measured with a digital anemometer (Lutron Digital Anemometer, AM-4201, range 0.4–30 m/s, accuracy  $\pm 1\%$ ) and four temperature sensors (PT 100RTD

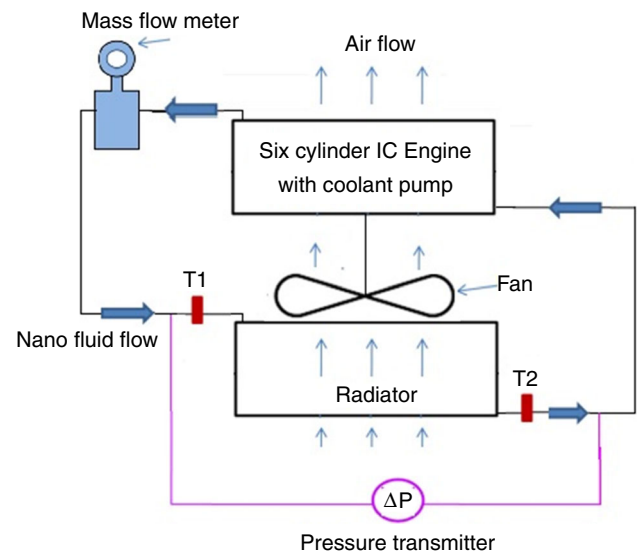


**Fig. 3** Schematic view of experimental setup

with range =  $-200$  to  $+850$  °C,  $\pm 0.15$  °C accuracy), respectively. Two temperature sensors were hung both in inlet side and outlet side of air flow across the radiator to measure air temperature. The reasons for choosing the radiator with elliptically cross-sectioned vertical tube and parallel plate fins are lower drag force compared to round tubes, minimum flow resistance and usage in heavy vehicles. The coolant flows downward, and air is flowing across the vertical tubes. The photographic view of the experimental setup with measuring instruments is shown in Fig. 4. The geometry and surface properties of the radiator are given in Tables 2 and 3, respectively.

## Experimental procedure

The engine was warmed up with no load, and load was increased to maximum efficiency condition. The engine was allowed to reach equilibrium for speed and load. The flow rate of 0.2% fly ash nanofluid coolant was adjusted to coolant Reynolds number 4000 with a constant air flow

**Fig. 4** Photographic view of experimental setup. A-radiator, B-outlet pressure gauge, C-flow meter, D-inlet pressure gauge, E-six-cylinder engine, F-temperature indicator switch, G-digital temperature indicator, H-thermocouple on the fin surface, M-thermocouple on the radiator tube

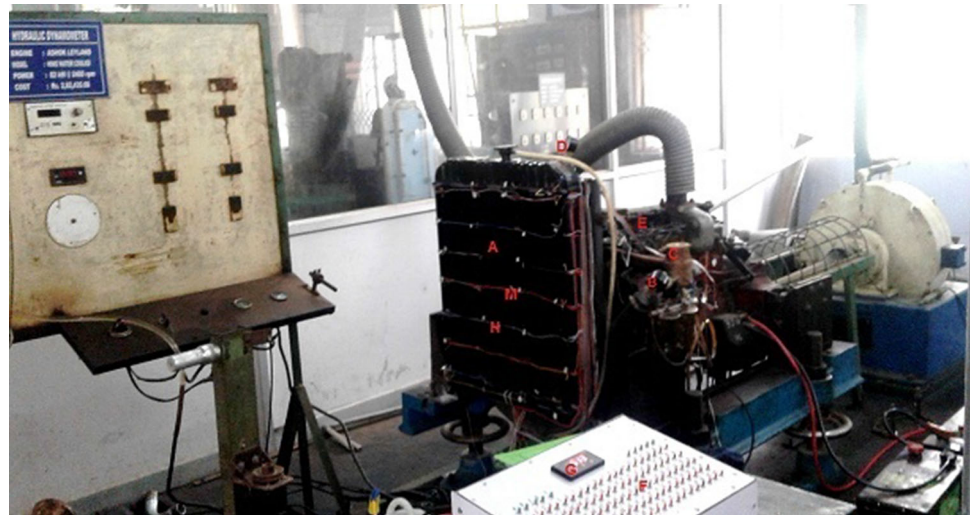


**Table 2** Radiator tube and fin dimensions

<i>Radiator tube dimensions</i>	
Core height × width × depth	630 mm × 550 mm × 48 mm
Tube material and thickness	Brass and 0.5 mm
Thermal conductivity	110.7 W m <sup>-1</sup> K <sup>-1</sup>
Tube arrangement, liner pitch and lateral pitch	Staggered, 10 mm and 5 mm
Number of rows and number of tubes	3 and 194
<i>Radiator fin dimensions</i>	
Fin type	Continuous flat fin
Fin material	Copper
Fin thickness	0.8 mm
Fin pitch	6.24 fins/inch
Total number of fins	171

**Table 3** Radiator surface properties

Surface characteristics	Air-side	Coolant side
Hydraulic diameter ( $D_h$ )	0.0035 m	0.00923 m
Free flow area per unit frontal area ( $\beta$ )	0.5558	0.2328
Heat transfer area per unit total volume ( $\alpha$ )	385 m <sup>2</sup> /m <sup>3</sup>	183 m <sup>2</sup> /m <sup>3</sup>

rate. The engine was allowed to reach steady state, and readings such as nanofluid flow rate, inlet, outlet temperature, the pressure difference across the radiator, the speed of the engine, air velocity, air temperatures at the inlet and outlet were observed. The tests were repeated for nanofluid Reynolds number range 4000–8000. The same tests were repeated for a nanofluid volume concentration range from 0.2 to 2% and base fluid. From the experimental readings heat transfer parameters, frictional performance parameters

and exergy parameters of the radiator were estimated by using Eqs. (8–26) and behavior of fly ash nanofluids was compared with base fluid.

### Data reduction for energy analysis

Heat transfer rate of nanofluid coolant calculated [25] by using the equation

$$Q = \dot{m}_c c_c (T_{c \text{ in}} - T_{c \text{ out}}) \quad (8)$$

Velocity of nanofluid coolant is determined [25] by the following equation

$$u_c = \frac{\dot{m}_c}{A_c} \quad (9)$$

Coolant side Reynolds number was calculated [21, 25, 26] as given in Eq. (10)

$$Re_c = \frac{\rho_c u_c d_{hc}}{\mu_c} \quad (10)$$

Air-side Reynolds number was estimated [25–27] by using Eq. (11)

$$Re_a = \frac{\rho_a u_a d_{ha}}{\mu_a} \quad (11)$$

Coolant side heat transfer coefficient was estimated [25] by the following Eq. (12)

$$h_c = \frac{Q}{A_c (T_B - T_w)} \quad (12)$$

Air-side heat transfer coefficient was obtained [25] as given in Eq. (13)

$$h_a = \frac{Q}{A_a (T_w - T_a)} \quad (13)$$

Overall efficiency of the radiator was determined [25] by using the equation

$$\eta_o = \left(\frac{A_f}{A_a}\right)\eta_f + 1 - \left(\frac{A_f}{A_a}\right) \quad (14)$$

Fin efficiency was obtained [25] by Eq. (15)

$$\eta_f = \frac{\tanh(mL)}{mL} \quad (15)$$

where

$$m = \sqrt{\frac{2h_a}{kt}} [25] \quad (16)$$

Overall heat transfer coefficient of the radiator (U) was estimated [25–27] from the following equation

$$\frac{1}{UA_a} = \frac{1}{\eta_o h_a A_a} + \frac{1}{h_c A_c} \quad (17)$$

Coolant pressure drop in the radiator was calculated [26, 28] by the using the following equation

$$\Delta p_c = \frac{\rho_c f_c H u_c^2}{2D_{hc}} \quad (18)$$

Volume flow rate of coolant was estimated [19, 29] as given in Eq. (19)

$$\dot{V}_c = \frac{\pi}{4} d_{hc} R e_c \frac{\mu_c}{\rho_c} \quad (19)$$

Coolant pumping power was determined [19, 21] by using Eq. (20)

$$P = \dot{V}_c \Delta p_c \quad (20)$$

Performance index of the radiator found out [19] by using the following equation

$$PI = \frac{Q}{P} \quad (21)$$

### Data reduction for exergy analysis

The exergy is the maximum useful work that can be obtained when a system at a particular equilibrium state moves toward thermodynamic equilibrium with the surroundings. Both energy and exergy analyses are needed for measuring radiator performance. The energy analysis measures the quantity of energy transfer, and exergy analysis measures the quality of energy transfer. The exergy depends on the state of system and surrounding. If the system reaches dead state, exergy becomes zero and the system could not deliver the work. The exergy destruction happened when heat is transferred with finite temperature difference and pressure drop due to friction. So that in heat exchanger the total exergy destruction rate is the sum of the frictional exergy destruction rate and thermal exergy destruction rate. The general exergy balance in a steady flow process can be defined [30–32] as

$$\sum E_{c\text{in}} - \sum E_{c\text{out}} = \sum E_{c\text{Des}} \quad (22)$$

The exergy loss of the coolant through the radiator tube was calculated [30, 33] by using the following equation

$$\sum E_{c\text{Des}} = Q - T_0 \left( \dot{m}_c C_{pc} \ln \left( \frac{T_{c\text{in}}}{T_{c\text{out}}} \right) - \dot{m}_c \left( \frac{\Delta p_c}{\rho_c T_0} \right) \right) \quad (23)$$

The exergy gain by the air flowing in the radiator tube was determined [30, 33] by using Eq. (24)

$$\sum E_{\text{air gain}} = Q - T_0 \left( \dot{m}_a C_{pa} \ln \left( \frac{T_{a\text{out}}}{T_{a\text{in}}} \right) - \dot{m}_a R \ln \left( \frac{p_{a\text{in}}}{p_{a\text{out}}} \right) \right) \quad (24)$$

The exergy destruction rate in non-dimensional form [30, 31] was determined as given in Eq. (25)

$$e = \left[ \frac{T_{c\text{out}} - T_{c\text{in}}}{T_0} - \ln \left( \frac{T_{c\text{out}}}{T_{c\text{in}}} \right) \right] + \left[ \frac{\Delta p_c}{\rho_c C_{pc} T_0} \right] = e(T) + e(p) \quad (25)$$

The second law efficiency ( $\eta_{II}$ ) of an automobile radiator is defined as the ratio exergy gain of the air flowing across the radiator to the exergy lost by the coolant while flowing through radiator tubes, and it was calculated [19] by using the following equation

$$\eta_{II} = \frac{\sum E_{\text{air gain}}}{\sum E_{c\text{Des}}} \quad (26)$$

### Uncertainty analysis

Errors are associated with various primary experimental measurements and the calculations of performance parameters. The factors influencing the amount of errors and uncertainties are selection of instrument, method of calibration, environment of experiment, methods of observation of readings and test planning. Uncertainty analysis is needed for research experiments to provide accurate results and findings.

In the present investigation, the maximum possible errors in performance parameters such as the overall heat transfer coefficient, heat transfer, pumping power and performance index were calculated by using the principle of root-mean-square method. The general formula to find maximum possible error using root-mean-square method is

$$\Delta R = \left[ \left( \frac{\partial R}{\partial x_1} \Delta x_1 \right)^2 + \left( \frac{\partial R}{\partial x_2} \Delta x_2 \right)^2 + \dots + \left( \frac{\partial R}{\partial x_n} \Delta x_n \right)^2 \right]^{1/2} \quad [34] \quad (27)$$

The uncertainty in determining heat transfer rate was calculated by using Eq. (28) [33, 34]

$$\partial Q = \sqrt{\left(\frac{\partial Q}{\partial m} \partial m\right)^2 + \left(\frac{\partial Q}{\partial c_p} \partial c_p\right)^2 + \left(\frac{\partial Q}{\partial T_{c\text{in}}} \partial T_{c\text{in}}\right)^2 + \left(\frac{\partial Q}{\partial T_{a\text{in}}} \partial T_{a\text{in}}\right)^2} \tag{28}$$

The uncertainty in overall heat transfer coefficient was estimated by using Eq. (29) [33, 34]

$$\partial U = \sqrt{\left(\frac{\partial U}{\partial h_c} \partial h_c\right)^2 + \left(\frac{\partial U}{\partial h_a} \partial h_a\right)^2 + \left(\frac{\partial U}{\partial \eta_f} \partial \eta_f\right)^2} \tag{29}$$

The uncertainty in pumping power was calculated by using Eq. (30) [33]

$$\partial P = \sqrt{\left(\frac{\partial P}{\partial m} \partial m\right)^2 + \left(\frac{\partial P}{\partial \rho} \partial \rho\right)^2 + \left(\frac{\partial P}{\partial \Delta P} \partial \Delta P\right)^2} \tag{30}$$

The uncertainty in performance index was estimated by using Eq. (31) [33]

$$\partial (PI) = \sqrt{\left(\frac{\partial (PI)}{\partial Q} \partial Q\right)^2 + \left(\frac{\partial (PI)}{\partial P} \partial P\right)^2} \tag{31}$$

The uncertainty of measuring instruments and estimated quantities are given in Table 4.

### Results and discussion

In the present work, heat transfer parameters, frictional parameters and exergy parameters of a heavy vehicle radiator using fly ash nanofluids as the coolants for volume concentration range 0–2% were investigated. The experiments were conducted by keeping coolants Reynolds number ranges from 4000 to 8000 and keeping air-side Reynolds number to 5000. The influence of volume concentration on heat, friction and exergy performance was compared to base fluid and discussed.

#### Overall heat transfer coefficient

The influence of coolant Reynolds number on overall heat transfer coefficient for different loadings of fly ash nanoparticles (0–2% by volume) in base fluid is shown in Fig. 5. The result shows that the overall heat transfer coefficient is increasing with increase in nanofluid concentration and increase in the Reynolds number. In all concentration ranges and the Reynolds number ranges in the study, the overall heat transfer coefficient is higher than base fluid. The overall heat transfer coefficient is increased from 119 to 133 W m<sup>-2</sup> K<sup>-1</sup> (11.7%) when nanofluid volume concentration increased from 0 to 2% and keeping the coolant Reynolds number to 4000. But at coolant

**Table 4** Uncertainty of measuring instruments and estimated performance parameters

Measuring instruments/performance parameters	Uncertainty
Temperature sensor ( $\delta_T$ )	$\pm 0.15$ °C
Differential pressure transducer ( $\delta_{\Delta p}$ )	$\pm 0.1\%$
Coriolis type mass flow meter ( $\delta_m$ )	$\pm 0.1\%$
Digital anemometer ( $\delta_v$ )	$\pm 1\%$
Heat transfer rate ( $\delta_Q$ )	$\pm 4.81\%$
Overall heat transfer coefficient ( $\delta_U$ )	$\pm 3.69\%$
Pumping power ( $\delta_P$ )	$\pm 3.34\%$
Performance index ( $\delta_{PI}$ )	$\pm 5.10\%$

Reynolds number 8000 and for the same range of volume concentration (0–2%), the overall heat transfer coefficient is increased from 138 to 167 W m<sup>-2</sup> K<sup>-1</sup> (21%). The overall heat transfer coefficient is improved from 119 to 138 W m<sup>-2</sup> K<sup>-1</sup> (15.9%), 121 to 147 W m<sup>-2</sup> K<sup>-1</sup> (21.4%), 133 to 167 W m<sup>-2</sup> K<sup>-1</sup> (25.5%) for base fluid, 0.2%, 2% fly ash nanofluid, respectively, when the Reynolds number increased from 4000 to 8000. This shows that the overall heat transfer coefficient is increasing for both nanofluid volume concentration and the Reynolds number, but the increase is more for the Reynolds number variation compared to nanofluid concentration variation. This increase in overall heat transfer coefficient with the Reynolds number is the result of increase in velocity of coolant, Nusselt number, and the increase with % volume concentration is due to increase in thermal conductivity and the increase in specific heat of coolant with nanoparticles loading. The increase in overall heat transfer coefficient in the present study using fly ash nanofluid (21%) is comparatively higher than the previous studies [35, 36] on

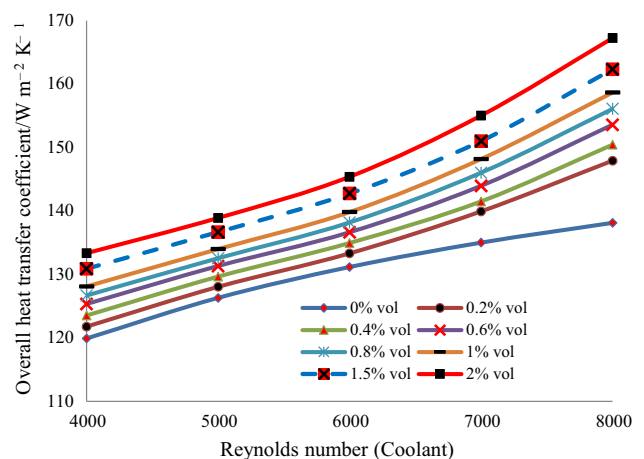


**Fig. 5** Influence of the Reynolds number (coolant) on overall heat transfer coefficient

automobile radiators using CuO (7%) and Fe<sub>2</sub>O<sub>3</sub> (9%) nanoparticles (about 2% by volume) in water/ethylene glycol base fluid.

### Heat transfer rate

The influence of % volume concentration (0–2%) of fly ash nanofluid and coolant Reynolds number on the heat transfer rate is shown in Fig. 6. It is found that the heat transfer rate is increasing with the increase in nanoparticles loading in base fluid and with the increase in the Reynolds number from 4000 to 8000. In the present study, the heat transfer is marginally increased from 12 to 18 kW (50%) when nanofluid volume concentration changed from 0 to 2% keeping the coolant Reynolds number 4000 and 16 kW to 23 kW (43.7%) when nanofluid volume concentration increased from 0 to 2% keeping the coolant Reynolds number 8000. The heat transfer is improved from 12 to 16 kW (33.3%) and 18 to 23 kW (27.4%) for base fluid and 2% volume concentration nanofluid, respectively, when the Reynolds number increased from 4000 to 8000. Nguyen et al. [8], conducted similar experiments on radiators and reported 40% heat transfer improvement at 6.8 vol% Al<sub>2</sub>O<sub>3</sub> nanoparticles in water. Few other previous investigations on automobile radiators reported that the maximum enhancement in heat transfer for 2% CuO/water [10] (20%), whereas that for 0.65% Fe<sub>2</sub>O<sub>3</sub>/water [11] (11.5%), for 2% SiO<sub>2</sub>/60%EG-40%water [12] (4.8%) and for 5% TiO<sub>2</sub>/water [13] (33%). The heat transfer characteristics of the fly ash nanofluid (0–2%) used in the present study are superior to base fluid, other fluids used in previous investigations, and it could be used as an automobile radiator coolant for better energy performance.

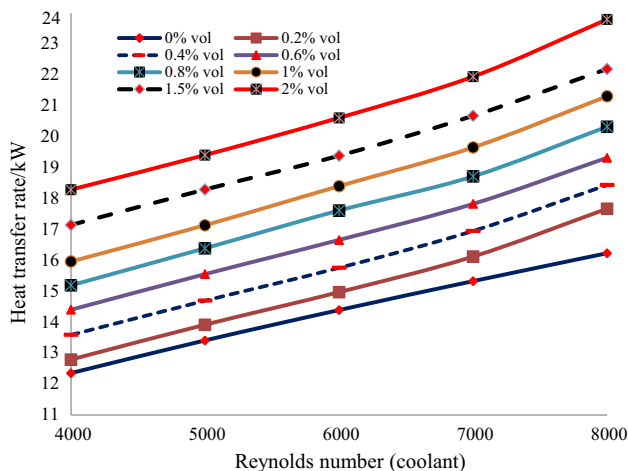


**Fig. 6** Influence of the Reynolds number (coolant) on heat transfer rate of radiator

### Pumping power

The frictional performance of the radiators is investigated by finding the outlet pressure of coolant and pumping power for 0%, 0.2%, 0.4%, 0.6%, 0.8%, 1%, 1.5% and 2% volume concentration of fly ash nanofluid for coolant Reynolds number range 4000–8000 keeping constant air Reynolds number 5000. The mass flow rate of nanofluid coolant increases with increases in volume fraction. The influence of nanoparticle concentration on pumping power for the Reynolds number ranges 4000–8000 was studied and plotted in Fig. 7. The graph shows that increase in fly ash volume concentration increases the pressure drop and pumping power. The maximum increase in pumping power of 0.32 kW (50%) was observed for 2% volume fly ash nanoparticle addition in base fluid tested with the Reynolds number 8000. The increase in pumping power in the present experimental investigation using fly ash is marginally higher than previous researches on automobile radiators which reported [37] 12.13% increase in pumping power when 2% copper nanoparticles are added in water/ethylene glycol base fluid. The study reveals that fly ash nanofluid requires more pumping power compared to other nanofluids and base fluid. But higher performance index at all % volume concentrations and all the Reynolds number ranges, environmental friendly and low cost of the fly ash nanofluid (0–2%) could favor its use as coolant in automobile radiators.

### Radiator performance index

The performance index of automobile radiators is the ratio of heat transfer rate to pumping power which indicates the effective improvement of heat transfer rate. Figure 8 explains the radiator performance index with 0–2% volume concentration of fly ash nanofluid in the Reynolds number

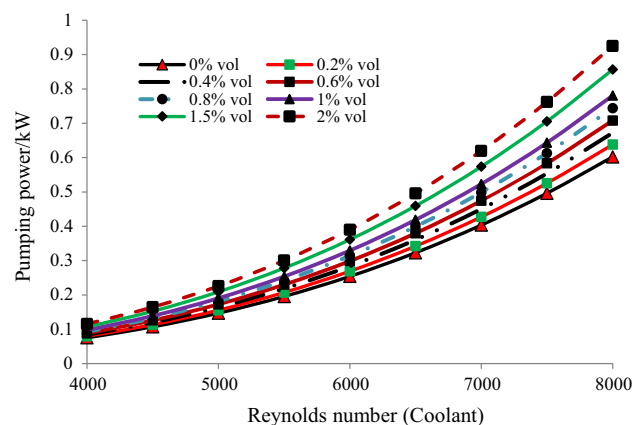


**Fig. 7** Influence of the Reynolds number (coolant) on pumping power of radiator



range considered and its variation with respect to coolant Reynolds number nanofluid concentration. It was observed that the performance index is increasing in the entire concentration range (0–2%) and the Reynolds number range (4000–8000) compared to base fluid. It is increasing with nanofluid concentration up to 0.2% and then slightly decreasing from 0.2 to 2% but not decreasing below base fluid. The performance index is decreasing with increase in the Reynolds number at all volume concentrations of nanofluids. The similar trends were reported by Sahoo et al. [19]. The reason for the decrease in performance index with an increase in the Reynolds number is due to the rate of increase of frictional power with increase in the Reynolds number more compared to rate of increase of heat transfer with increase in nanoparticles concentration. The increase in performance index in the entire concentration range (0–2%) and the Reynolds number range compared to base fluid indicates that up to 2% volume of fly ash nanoparticles could be added in base fluid (40% EG + 60 water) for increasing cooling performance of heavy vehicle radiators.

**Exergy destruction rate**

The variation of frictional, thermal and total exergy destruction rate, keeping the Reynolds number variation from 4000 to 8000 and fly ash nanoparticles concentration range 0.2–2% are shown in Figs. 9–11. The frictional exergy rate increases with the Reynolds number and nanoparticles concentration. This increase is because of an increase in viscosity and friction with the addition of nanoparticles in the nanofluid. The thermal exergy destruction rate decreases with increase in fly ash nanoparticle concentration and the Reynolds number which is due to increase in fly ash nanofluid thermal conductivity

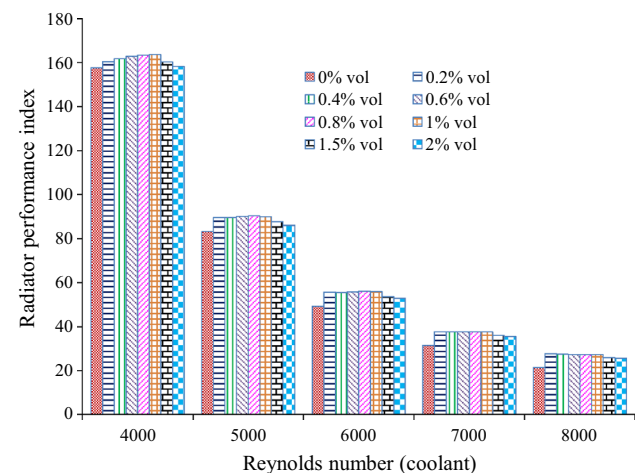


**Fig. 8** Influence of the Reynolds number (coolant) on radiator performance index

and Nusselt number. But compared to base fluid, the frictional exergy destruction rate, thermal exergy destruction rate and total exergy destruction rate are less for all concentrations of the nanofluid at all the Reynolds number values. The decrease in the total exergy destruction rate indicates that exergy performance of the radiator is improved by the addition of nanoparticles in base fluid. The results also indicate that frictional exergy destruction rate is less compared to thermal exergy destruction rate.

**Second law efficiency**

The curves in Fig. 12 explain that the second law efficiency of the radiator decreases (6.3%) with an increasing coolant Reynolds number from 4000 to 8000 for 2% volume and increases (3%) with fly ash nanofluid concentration (0–2%). The reason for this decrease in second law efficiency with the Reynolds number is due external and internal irreversibilities. The increase is due to increase in

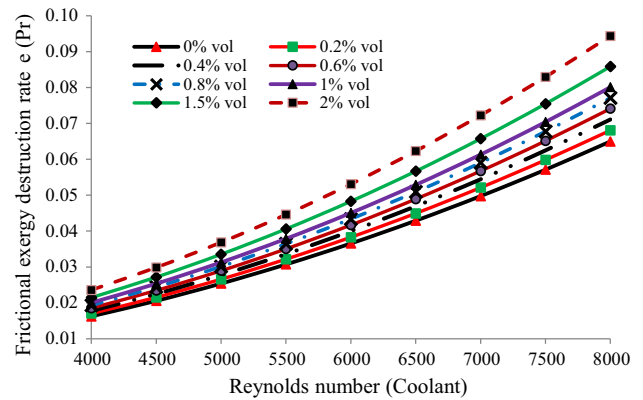


**Fig. 9** Influence of the Reynolds number (coolant) on frictional exergy destruction rate

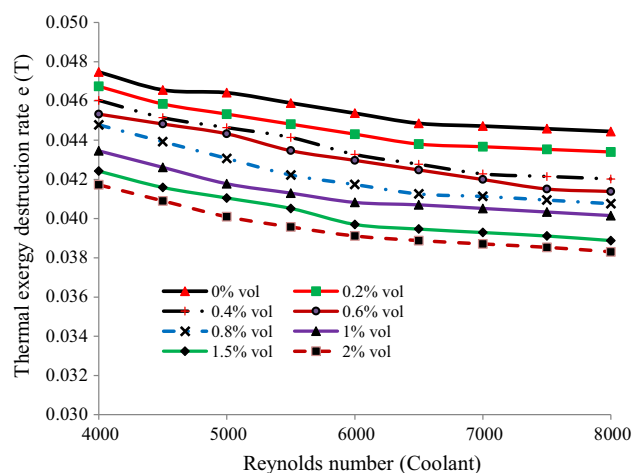


**Fig. 10** Influence of the Reynolds number (coolant) on thermal exergy destruction rate

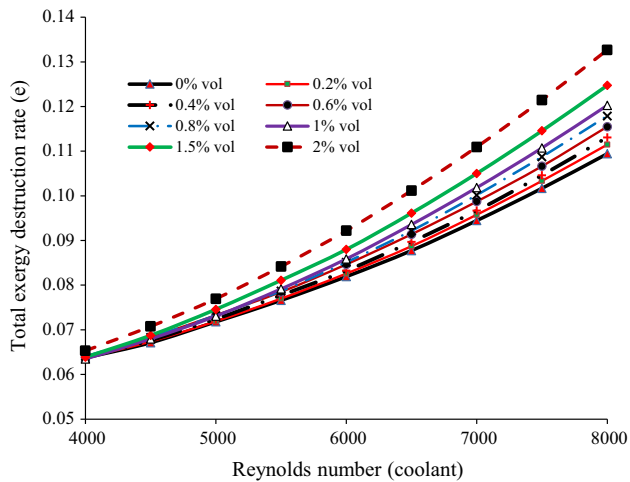


**Fig. 11** Influence of the Reynolds number (coolant) on total exergy destruction rate

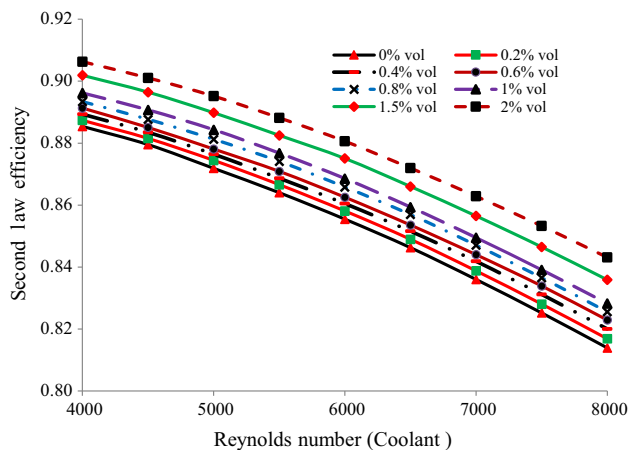


**Fig. 12** Influence of the Reynolds number (coolant) on second law efficiency

thermal capacity due to addition of nanoparticle in base fluid. The trend of second law efficiency of the present research is matched with Khaleduzzaman et al. [30] and Ghazikhani et al. [31].

## Conclusions

Thermodynamic analysis of fly ash nanofluid for automobile (heavy vehicle) radiators was carried out to investigate the effect of fly ash nanofluid volume concentration (0–2%), coolant Reynolds number (4000–8000) on overall heat transfer coefficient, heat transfer rate, pumping power, frictional exergy destruction rate, thermal exergy destruction rate, total exergy destruction rate and second law efficiency. The results of the analysis have given the following conclusions.

1. Increasing fly ash nanoparticles concentration (0–2%) in a base fluid (60% water + 40% ethylene glycol) increases overall heat transfer coefficient ( $29 \text{ W m}^{-2} \text{ K}^{-1}$  at the Reynolds number 8000), heat transfer rate (7 kW at the Reynolds number 8000) and pumping power (0.3 kW at the Reynolds number 8000) compared to base fluid in the entire Reynolds number range. But the increase in heat transfer (about 7 kW) is more compared to increase in pumping power (about 0.3 kW) in the Reynolds number range 4000–8000.
2. It is observed that the thermal exergy destruction rate decreases and frictional exergy destruction rate and total exergy destruction increase with the Reynolds number and with fly ash nanofluid concentration.
3. The second law efficiency decreases with increasing the Reynolds number at all nanofluid concentrations and increases with nanofluid concentration in the Reynolds number range 4000–8000.
4. In energy, exergy point of view the fly ash nanoparticles with average particle size 50 nm can be added up to 2% volume concentration in the conventional (40:60-EG/water) coolant to improve overall performance of the heavy vehicle radiators.

## References

1. Yao ZP, Wang XG. The cooling and heat transfer of vehicles. Beijing: Beijing Institute of Technology Press; 2001.
2. Hongjie N. China internal combustion engine industry year book. Shanghai: Shanghai Jiao Tong University Press; 2005.
3. Ali M, El-Leathy AM, Al-Sofyany Z. The Effect of Nanofluid Concentration on the Cooling System of Vehicles Radiator. *Advances in Mechanical Engineering*. 2014;6:1–13.
4. Naraki M, Peyghambarzadeh SM, Hashemabadi SH, Vermahmoudi Y. Parametric study of overall heat transfer coefficient of CuO/water nanofluids in a car radiator. *Int J Therm Sci*. 2013;66:82–90.
5. Godson L, Raja B, Lal DM, Wongwises S. Enhancement of heat transfer using nanofluids—an overview. *Renew Sustain Energy Rev*. 2010;14(2):629–41.
6. Mints HA, Roy G, Nguyen CT, Doucet D. New temperature dependent thermal conductivity data for water-based nanofluids. *Int J Therm Sci*. 2009;48:363–71.
7. Peyghambarzadeh SM, Hashemabadi SH, Seifi Jamnani M, Hoseini SM. Improving the cooling performance of automobile radiator with  $\text{Al}_2\text{O}_3$ /water nanofluid. *Appl Therm Eng*. 2011;31:1833–8.
8. Nguyen CT, Roy G, Gauthier C, Galanis N. Heat transfer enhancement using  $\text{Al}_2\text{O}_3$ -water nanofluid for an electronic cooling system. *Appl Therm Eng*. 2007;27:1501–6.
9. Heris SZ, Etemad SG, Esfahany N. Experimental investigation of oxide nanofluids laminar flow convective heat transfer. *Int Commun Heat Mass Transf*. 2006;33(4):529–35.
10. Li Q, Xuan Y. Experimental investigation of transport properties of nanofluids, Buxan Wang Edition. Heat transfer science and technology. Beijing: Higher Education Press; 2000.

11. Vermahmoudi Y, Peyghambarzadeh SM, Hashemabadib SH, Narakia M. Experimental investigation on heat transfer performance of Fe<sub>2</sub>O<sub>3</sub>/water nanofluid in an air-finned heat exchanger. *Eur J Mech B Fluids*. 2011;44:32–41.
12. Kulkarni DP, Namburu PK, Bargar HE, Das DK. Convective heat transfer and fluid dynamic characteristics of SiO<sub>2</sub> ethylene glycol/water nanofluid. *Heat Transf Eng*. 2008;29:1027–35.
13. Murshed SMS, Leong KC, Yang C. Enhanced thermal conductivity of TiO<sub>2</sub>-water based nanofluids. *Int J Therm Sci*. 2005;44:367–73.
14. Dhinesh Kumar D, Valan Arasu A. A review on preparation, characterization, properties and applications of nanofluids. *Renew Sustain Energy Rev*. 2016;60:21–40.
15. Sozen A, Ibrahim Variyenli H, Bahadir Ozdemir M, Guru M, Aytac I. Heat transfer enhancement using alumina and fly ash nanofluids in parallel and cross-flow concentric tube heat exchangers. *J Energy Inst*. 2016;89(3):414–24.
16. Yilmaz M, Sara ON, Karsli S. Performance evaluation criteria for heat exchangers based on second law analysis. *Int J Exergy*. 2001;1(4):278–94.
17. Gupta P, Kush PK, Tiwari A. Second law analysis of counter flow cryogenic heat exchanger in presence of ambient heat-in-leak and longitudinal conduction through wall. *Int J Heat Mass Transf*. 2007;9:4754–66.
18. Gupta A, Das SK. Second law analysis of cross-flow heat exchanger in the presence of axial dispersion in one fluid. *Energy*. 2007;32:664.
19. Sahoo RR, Ghosh P, Sarkar J. Performance comparison of various coolants for louvered fin tube automobile radiator. *Therm Sci*. 2017;21(6B):2871–81.
20. Bashirnezhad K, Rashidi MM, Yang Z, Bazri S, Yan WM. A comprehensive review of last experimental studies on thermal conductivity of nanofluids. *J Therm Anal Calorim*. 2015;122:863–84.
21. Alosious S, Sarath SR, Anjan RN, Krishnakumar K. Experimental and numerical study on heat transfer enhancement of flat tube radiator using Al<sub>2</sub>O<sub>3</sub> and CuO nanofluids. *Heat Mass Transf*. 2017;53:3545–63. <https://doi.org/10.1007/s00231-017-2061-0>.
22. Vajjha RS, Das DK, Kulkarni DP. Development of new correlations for convective heat transfer and friction factor in turbulent regime for nanofluids. *Int J Heat Mass Transf*. 2010;53:4607.
23. Zyla Gawel. Viscosity and thermal conductivity of MgO-EG nanofluids experimental results and theoretical models predictions. *J Therm Anal Calorim*. 2017;29:171–80.
24. Mohanraj M, Jayaraj S, Muraleedharan C. Applications of artificial neural networks for thermal analysis of heat exchangers—a review. *Int J Therm Sci*. 2015;90:150–72.
25. Selvam C, Solaimalai Raja R, Mohan Lal D, Harish S. Overall heat transfer coefficient of an automobile radiator with grapheme based suspensions. *Int J Heat Mass Transf*. 2017;115:580–8.
26. Chayulu DG, Singh G, Sharma JK. Performance evaluation of a radiator in a diesel engine—a case study. *Appl Therm Eng*. 1999;19:625–39.
27. Vasu V, Krishna KR, Kumar ACS. Application of nanofluids in thermal design of compact heat exchanger. *Int J Nanotechnol Appl*. 2008;2(1):75.
28. Tsai TH, Chein R. Performance analysis of nanofluid-cooled microchannel heat sinks. *Int J Heat Fluid Flow*. 2007;28:1013–26.
29. Sarkar J, Tarodiya R. Performance analysis of louvered fin tube automotive radiator using nanofluids as coolants. *Int J Nanomanuf*. 2013;9(1):51.
30. Khaleduzzaman SS, Sohail MR, Mahbulul IM, Akash BA, Selvaraj J. Energy and exergy analysis of alumina-water nanofluid for an electronic liquid cooling system. *Int Commun Heat Mass Transf*. 2014;57:118–27.
31. Ghazikhani M, Khazaei I, Monazzam SMS, Takdehghan H. Exergy destruction analysis of a vertices generator in a gas liquid finned heat exchanger: an experimental study. *Heat Mass Transf*. 2016;52:2531–9.
32. Mohanraj M, Jayaraj S, Muraleedharan C. Exergy assessment of a direct expansion solar assisted heat pump working with R22 and R407C/LPG mixture. *Int J Green Energy*. 2010;7:65–83.
33. Suha OM, Alper R. Experimental performance investigation of a shell and tube heat exchanger by exergy based sensitivity analysis. *Heat Mass Transf*. 2016;52:1117–23.
34. Moffat RJ. Describing the uncertainties in experimental results. *Exp Therm Fluid Sci*. 1988;1:3–17.
35. Peyghambarzadeh SM, Hashemabadi SH, Hoseini SM, SeifiJamnani M. Experimental study of heat transfer enhancement using water/ethylene glycol based nanofluids as a new coolant for car radiators. *Int Commun Heat Mass Transf*. 2011;38:1283–90.
36. Peyghambarzadeh SM, Hashemabadi SH, Mi N, Vermahmoudi Y. Experimental study of overall heat transfer coefficient in the application of dilute nanofluids in the car radiator. *Appl Therm Eng*. 2013;52:8–16.
37. Leong KY, Saidur R, Kazi SN, Mamun AH. Performance investigation of an automotive car radiator operated with nanofluid based coolants (nanofluid as a coolant in a radiator). *Appl Therm Eng*. 2010;30:2685–92.